I&EC research
Industrial & Engineering Chemistry Research

Article

pubs.acs.org/IECR

State and Parameter Estimation in Distributed Constrained Systems. 1. Extended Kalman Filtering of a Special Class of Differential-Algebraic Equation Systems

Parham Mobed,[†] Sudhakar Munusamy,[†] Debangsu Bhattacharyya,[‡] and Raghunathan Rengaswamy*[,†,§]

[†]Department of Chemical Engineering, Texas Tech University, Lubbock, Texas 79409, United States
[‡]Department of Chemical Engineering, West Virginia University, Morgantown, West Virginia 26506, United States
[§]Department of Chemical Engineering, Indian Institute of Technology, Madras, Chennai 600 036, India

ABSTRACT: State and parameter estimation plays an important role in many different engineering fields. Estimation of systems described by linear and nonlinear differential equations has been very well studied in the literature. Work in the past decade has been geared toward efficiently extending these algorithms to constrained systems. Of recent interest is the evaluation of state estimation techniques for differential-algebraic equation (DAE) systems. The algebraic equations in these studies are exact, an example being the mole fractions adding to unity. However, there are situations where algebraic equations can be of both certain and uncertain types. In this paper, we propose a modified extended Kalman filter (EKF) approach that can handle uncertainties in both differential and algebraic equations, and equality constraints. We also show the importance of this work in estimation of mole fraction, temperature, and pressure profiles in a water gas shift reactor. The impact of location and type of measurements on the estimation accuracy is also studied.

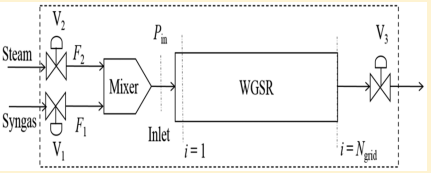

1. INTRODUCTION

Differential-algebraic equation (DAE) systems often arise in modeling of physical and mechanical systems, such as robotics, chemical processes, electrical circuits, and so on. DAE systems, which are also called descriptor systems, can be viewed as ordinary differential equations (ODEs) that are coupled with algebraic equations through additional algebraic states. In general, both the differential and algebraic equations can be linear or nonlinear. Although the dynamic behavior is modeled by ODEs, the presence of algebraic constraints results in some complications while solving the DAE systems. State estimation of linear and nonlinear ODEs has been studied thoroughly in the literature, and several techniques are available for state estimation, including, but not limited to, Kalman filter (KF), extended Kalman filter (EKF), unscented Kalman filter (UKF), ensemble Kalman filter (EnKF), particle filters, and so on.[1] The Kalman filter is an estimator of linear stochastic ODEs, where the term "stochastic" represents the presence of process and measurement noises. Kalman filter is optimal when the noise is assumed as Gaussian white noise. Although Kalman filter is optimal for linear systems, an extension of KF is suboptimal when applied to nonlinear systems.[2] The idea of extended Kalman filter (EKF) is based on local linearization of the nonlinear equations and application of the linear Kalman filter framework. At first glance, it seems that by converting the DAE to an implicit ODE, state estimation can be performed using the KF or EKF framework, as it is used for implicit ODE systems. However, unlike ODE systems, there is a necessity of generation of consistent initial guesses that respect the algebraic constraints. Further, DAEs are characterized by the index of the system, which is the number of differentiations that are required to convert a DAE system into a fully implicit ODE. As a result, state estimation techniques for ODEs cannot be directly extended to DAE systems.[3]

The index of a DAE represents the difficulty in the numerical treatment of such systems. DAEs of index zero and one are considered to be the easiest for numerical treatment compared to higher index systems.[4] The systems considered in this work are all assumed to be index-1 DAEs. A literature search indicates extensive work on applying KF to linear DAEs, see refs 5−10, though there is very little work on implementation of EKF on nonlinear DAEs.[1,11] For applying EKF to DAE systems, Becerra et al.[11] proposed a modified EKF for DAE systems. In their approach, the DAE is converted to an implicit ODE and the nonlinear equations are linearized locally, and Kalman filter computations are performed at each sampling time, while the error covariance matrix is updated for differential states. A disadvantage of this approach is that the effects of prior algebraic state estimates and measurements from algebraic states are ignored and updated algebraic state estimates are obtained by solving the algebraic equations after updated differential state estimates are computed.[1] Further, measurements of the algebraic states cannot be directly included in this framework. To address these disadvantages, in our previous work, an approach was proposed that takes into account the effect of prior algebraic states and accommodates the measurements from the algebraic states in the framework.[1]

Received: July 22, 2016
Revised: October 2, 2016
Accepted: November 28, 2016
Published: November 28, 2016

DOI: 10.1021/acs.iecr.6b02796
Ind. Eng. Chem. Res. 2017, 56, 206−215

One of the difficulties in state estimation of DAEs is addressing the white noise term in the algebraic equations, as the derivative of white noise is not well-defined.[12] For linear systems, researchers have proposed different approaches to address this problem. For instance, Campbell[13] suggested the use of a band limited noise filter and in turn compromised the optimality of the Kalman filter. Schon et al.[14] explained the transformation of the DAE into a state space form and the conditions under which the derivative of white noise in algebraic equations can be avoided in state-space form. Darouach et al.[6] avoided the presence of the white noise derivative by decomposing the filtering problem into two subproblems: (i) computing the estimates and error covariance of differential states, and (ii) using them in computation of estimates and error covariance of algebraic states.

In almost all of the works that consider EKF for nonlinear DAEs, the algebraic equations are noise-free and the process noise is considered only in the differential equations. However, in practice, algebraic equations are not always exact and they might themselves be uncertain. This is particularly true when simplifying correlations are used in the modeling framework. This poses a problem because when the algebraic equations are differentiated to convert a DAE system to an implicit ODE system, white noise will have to be differentiated. Therefore, algebraic equations must be certain for differentiation to be meaningful. In this work, we address these issues by proposing a modification to the EKF to handle constrained DAEs of index-1 with uncertainties in both differential and algebraic equations. Further, we propose a modified EKF that can address exact algebraic linear equality constraints.

In the proposed work, the error covariance matrix is written as a 4-block matrix with separate square blocks for differential and algebraic variables, respectively. Since the DAE is of index-1, the algebraic equations are written in terms of the differential variables and the error covariance in the corresponding covariance matrix is updated by linear or nonlinear transformation of the error covariance of the differential equations. This avoids the differentiation of algebraic equations and makes the filter practical. The following sections are organized as follows. First, the currently available state estimation techniques for DAEs in the absence of uncertainties in algebraic variables are reviewed in Section 2. In Section 3, the EKF formulation from Section 2 is modified to account for exact equality constraints. Section 4 shows the performance of the proposed estimator on two examples, a simple example system and a water gas shift reactor.

2. STATE ESTIMATION OF DAE SYSTEMS

2.1. Problem formulation. Consider the following stochastic nonlinear discrete-time DAE system with discrete measurements sampled at intervals of Δt

$$\begin{aligned} x_{k+1} &= x_k + \int_{k\Delta t}^{(k+1)\Delta t} f(x(t), z(t))dt + \omega_{k+1} \\ g(x_{k+1}, z_{k+1}) &= 0 \\ y_{k+1} &= h(x_{k+1}, z_{k+1}) + \nu_{k+1} \\ \omega &\sim N(0, Q) \qquad \nu \sim N(0, R) \end{aligned} \tag{1}$$

where $x_{k+1} \in \mathbb{R}^{m\times 1}$ and $z_{k+1} \in \mathbb{R}^{p\times 1}$ are the differential and algebraic states at interval $(k+1)$, respectively; and $Q \in \mathbb{R}^{m\times m}$ and $R \in \mathbb{R}^{p\times p}$ are known covariance matrices.

2.2. Propagation. Let $\hat{x}_{k|k}$ and $\hat{z}_{k|k}$be the updated differential and algebraic states estimates at time $t = k\Delta t$ using the information available up to and including the k^{th} measurement sample, respectively. The predicted states, $\hat{x}_{k+1|k}$ and $\hat{z}_{k+1|k}$, are obtained by integrating the DAE system in eq 1. Let $P_{k|k}$ be the error covariance matrix of updated estimates; the predicted error covariance, $P_{k+1|k}$, is obtained by first linearizing the nonlinear system in eq 1 around the updated differential and algebraic states ($\hat{x}_{k|k}$ and $\hat{z}_{k|k}$) and by second differentiating the algebraic equations in eq 1 to convert the DAE into a continuous implicit ODE. Therefore, augmenting the resulting system as

$$\begin{bmatrix} \dot{x} \\ \dot{z} \end{bmatrix} = \begin{bmatrix} A & B \\ -D^{-1}CA & -D^{-1}CB \end{bmatrix} \begin{bmatrix} x \\ z \end{bmatrix} = A^{aug}x^{aug} \tag{2}$$

where the superscript *"aug"* represents the augmented form (i.e., $x^{aug} = \begin{bmatrix} x \\ z \end{bmatrix}$) and the Jacobian matrix around the $\hat{x}_{k|k}$ is evaluated as

$$J = \begin{bmatrix} A & B \\ C & D \end{bmatrix} = \begin{bmatrix} \frac{\partial f}{\partial x} & \frac{\partial f}{\partial z} \\ \frac{\partial g}{\partial x} & \frac{\partial g}{\partial z} \end{bmatrix}_{\hat{x}_{k|k}, \hat{z}_{k|k}} \tag{3}$$

The transition matrix, calculated as $\Phi = \exp(J\Delta t)$, is used to obtain the predicted error covariance by

$$P_{k+1|k} = \phi P_{k|k}\phi^T + \Gamma Q_{k+1}\Gamma^T \tag{4}$$

where

$$\Gamma = \begin{bmatrix} I \\ -D^{-1}C \end{bmatrix} \tag{5}$$

2.3. Correction. In the update step of EKF, the augmented states are updated as

$$\hat{x}^{aug}_{k+1|k+1} = \hat{x}^{aug}_{k+1|k} + K_{k+1}(y_{k+1} - h(\hat{x}^{aug}_{k+1|k})) \tag{6}$$

only the differential part of the estimated augmented states is retained and the algebraic part is obtained by solving

$$g(\hat{x}_{k+1|k+1}, \hat{z}_{k+1|k+1}) = 0 \tag{7}$$

The updated covariance matrix is obtained by

$$P_{k+1|k+1} = (I - K_{k+1}H_{k+1})P_{k+1|k} \tag{8}$$

where in the update step, H_{k+1} is the linearized measurement model evaluated at $\hat{x}^{aug}_{k+1|k}$ and K_{k+1} is the Kalman gain matrix calculated by

$$\begin{aligned} K_{k+1} &= P_{k+1|k}H^T_{k+1}(H_{k+1}P_{k+1|k}H_{k+1} + R_{k+1})^{-1} \\ &= (P^{-1}_{k+1|k} + H^T_{k+1}R^{-1}_{k+1}H_{k+1})^{-1}H^T_{k+1}R^{-1}_{k+1} \end{aligned} \tag{9}$$

Note that these equations are written for an augmented system, except for eq 7, where the algebraic part only is calculated.

3. EQUALITY CONSTRAINED STATE ESTIMATION OF UNCERTAIN NONLINEAR DAES

In practice, not all the algebraic equations that describe the behavior of a physical system are exact and additional information about the dynamic system may be available. If the algebraic equations are not exact, uncertainties must be considered in these equations to more closely represent the real behavior.

DOI: 10.1021/acs.iecr.6b02796
Ind. Eng. Chem. Res. 2017, 56, 206−215

Therefore, one could model uncertainties in the algebraic equations also as Gaussian random variables with known statistical properties. Moreover, if additional information about the system represents an equality constraint, which the system variables must satisfy, then this information must be incorporated into the estimation framework. In this section, we propose enhancements to the EKF approach for DAE systems to address this class of problems. We believe that this class of systems is quite common in all engineering disciplines and particularly in chemical engineering, where the DAE models are likely to be uncertain in addition to the presence of exact equality constraints arising out of flow balances and summation of mole fractions. For example, a complex chemical reaction system with a number of unknown side reactions producing a small fraction of unconsidered chemical species will lead to nonzero deviations in the algebraic equations.

Most efforts in constrained Kalman filtering are geared toward linear systems with optimal filtering while nonlinearities in the system result in suboptimal and complicated filtering.[4] Currently, approximations are inevitable in filtering nonlinear systems and the estimates remain suboptimal. In constrained Kalman filtering of nonlinear models, one makes the assumptions that handling constraints in nonlinear models can be done similar to their linear counterparts. There are several ways in which equality constraints can be incorporated into the linear Kalman filter framework. An attractive approach is to reduce the number of variables by explicit substitution into the model equations. This approach has the advantage of reducing the constrained problem to a simpler unconstrained problem with lower computational load of the Kalman filter. However, in nonlinear cases, it might not always be possible to explicitly reduce the dependent variables as a function of the independent variables. Study on constrained filtering has shown that projecting the unconstrained estimates of the Kalman filter on the constraint surface accommodates ease of implementation, low computational cost, and flexibility compared to other approaches for both linear and nonlinear systems.[4] In this work, constraints are handled by approaching the problem using the same state estimates projection approach.

3.1. Problem formulation. The system of interest in this paper is as shown in eq 10.

$$\begin{aligned} &x_{k+1} = x_k + \int_{k\Delta t}^{(k+1)\Delta t} f(x(t), z(t))dt + G\omega_{k+1} \\ &g(x_{k+1}, z_{k+1}) + \gamma_{k+1} = 0 \\ &y_{k+1} = h(x_{k+1}, z_{k+1}) + \nu_{k+1} \\ &\omega \sim N(0, Q) \qquad \nu \sim N(0, R) \qquad \gamma \sim N(0, W) \\ &\textit{subject to: } Ex_{k+1}^{aug} = b \end{aligned} \tag{10}$$

where in addition to the assumptions for the system described in eq 1, $G \in \mathbb{R}^{m\times m}$ is a known matrix with rank $(G) = l < m$, $E \in \mathbb{R}^{l\times m+n}$ is the equality constraint with rank $(E) = l$, which can be split into $E = [E_x \;\; E_z]$, where $E_x \in \mathbb{R}^{l\times m}$ satisfies $E_xG = 0_{l\times m}$ and $E_z = 0_{l\times n}$, $b \in \mathbb{R}^{l\times 1}$ is a vector of equality constraint values, and $W \in \mathbb{R}^{n\times n}$ is a known covariance matrix. The estimation algorithm described previously is not applicable for the defined system. The main issue is that the white noise is not differentiable; therefore, the system cannot be converted into an implicit ODE as shown in eq 2.

Remark 2.1: Assume rank $(E) = m + n$; then, for all $k \geq 1$ the system is fully constrained and the updated states are calculated as $x_{k+1} = E^{-1}b$. If rank $(E) = m + n$, then E is square and invertible. Therefore, the constraint equation has a unique answer as $x_{k+1} = E^{-1}b$.

3.2. Propagation. Let $\hat{x}_{k|k}$ and $\hat{z}_{k|k}$ be updated differential and algebraic state estimates, respectively, at k^{th} time instant, and let P_k be the error covariance of the states. States are propagated by solving the DAE from the k^{th} time instant to the $k+1^{\text{th}}$ time instant to get $\hat{x}_{k+1|k}$ and $\hat{z}_{k+1|k}$. In what follows, the superscripts "c" and "st" represent the corrected and standard form, respectively. In order to propagate the covariance matrix, the DAE system is linearized around the $\hat{x}_{k|k}$ and $\hat{z}_{k|k}$ as

$$\dot{x} = Ax + Bz \tag{11}$$

$$Cx + Dz = 0 \tag{12}$$

where the coefficient matrix of the linearized form is simply the Jacobian evaluated at the operating point, $\hat{x}_{k|k}$, $\hat{z}_{k|k}$, similar to eq 3. Solving eq 12 in terms of z and rewriting eq 11 gives

$$z = -D^{-1}Cx \tag{13}$$

$$\dot{x} = (A - BD^{-1}C)x \tag{14}$$

Based on differential and algebraic variables, the error covariance matrix can be split into

$$P_{k+1|k} = \begin{bmatrix} P_{k+1|k}^{xx} & P_{k+1|k}^{xz} \\ P_{k+1|k}^{zx} & P_{k+1|k}^{zz} \end{bmatrix} \tag{15}$$

The error covariance of differential states is calculated as

$$P_{k+1|k}^{xx} = \phi P_{k|k}^{xx} \phi^T + GQG^T \tag{16}$$

where Φ is the transition matrix of differential states and is obtained as

$$\phi = e^{(A-BD^{-1}C)\Delta t} \tag{17}$$

The error covariance of algebraic states is propagated as

$$P_{k+1|k}^{zz} = (D^{-1}C)P_{k+1|k}^{xx}(D^{-1}C)^T + D^{-1}WD^{-1^T} \tag{18}$$

Since the algebraic states are linear transformations of the differential states, the error covariance between differential and algebraic states is propagated as a linear transformation of the error covariance of differential states as

$$P_{k+1|k}^{xz} = P_{k+1|k}^{xx}(D^{-1}C)^T \tag{19}$$

$$P_{k+1|k}^{zx} = (D^{-1}C)P_{k+1|k}^{xx} \tag{20}$$

3.3. Propagation. The updated augmented state estimates are obtained by solving the following minimization problem

$$\begin{aligned} \min_{\hat{x}_{k+1|k+1}^{aug,c}} \; &(\hat{x}_{k+1|k+1}^{aug,c} - \hat{x}_{k+1|k}^{aug})^T P_{k+1|k}^{-1}(\hat{x}_{k+1|k+1}^{aug,c} - \hat{x}_{k+1|k}^{aug}) \\ &+ (y_{k+1} - H\hat{x}_{k+1|k+1}^{aug,c})^T R^{-1}(y_{k+1} - H\hat{x}_{k+1|k+1}^{aug,c}) \end{aligned} \tag{21}$$

subject to the state constraints

$$E\hat{x}_{k+1|k+1}^{aug,c} = b \tag{22}$$

where $\hat{x}_{k+1|k+1}^{aug,c}$ is the augmented updated state estimates (i.e., $\hat{x}_{k+1|k+1}^{aug,c} = \begin{bmatrix} \hat{x}_{k+1|k+1}^{c} \\ \hat{z}_{k+1|k+1}^{c} \end{bmatrix}$) that satisfies the state constraints.

DOI: 10.1021/acs.iecr.6b02796
Ind. Eng. Chem. Res. 2017, 56, 206−215

Remark 2.2: In the absence of any constraints, the optimization problem is similar to the problem investigated in the work of Vachhani et al.[15] and the solution to the optimization problem for all $k \geq 1$ is given by standard KF.

Proof: The proof is described in the work of Vachhani et al.[15]

The optimization problem is solved using the standard Lagrange multiplier technique, where the Lagrangian is defined as

$$\begin{aligned} &L(\hat{x}^{aug,c}_{k+1|k+1}, \lambda) \\ &= (\hat{x}^{aug,c}_{k+1|k+1} - \hat{x}^{aug}_{k+1|k})^T P_{k+1|k}{}^{-1} \\ &\quad (\hat{x}^{aug,c}_{k+1|k+1} - \hat{x}^{aug}_{k+1|k}) \\ &+(y_{k+1} - H\hat{x}^{aug,c}_{k+1|k+1})^T R^{-1}(y_{k+1} - H\hat{x}^{aug,c}_{k+1|k+1}) \\ &\quad + \lambda^T(E\hat{x}^{aug,c}_{k+1|k+1} - b) \end{aligned} \tag{23}$$

The necessary conditions for $\hat{x}^{aug,c}_{k+1|k+1}$ minimizing eq 23 are

$$\begin{aligned} \frac{\partial L}{\partial \hat{x}^{aug,c}_{k+1|k+1}} &= 2P_{k+1|k}{}^{-1}(\hat{x}^{aug,c}_{k+1|k+1} - \hat{x}^{aug}_{k+1|k}) - 2H^T \\ &\quad R^{-1}(y_{k+1} - H\hat{x}^{aug,c}_{k+1|k+1}) + E^T\lambda \\ &= 0 \end{aligned} \tag{24}$$

$$\frac{\partial L}{\partial \lambda} = E\hat{x}^{aug,c}_{k+1|k+1} - b = 0 \tag{25}$$

Solving eq 24 for $\hat{x}^{a,c}_{k+1|k+1}$ after some manipulations yields

$$\begin{aligned} \hat{x}^{aug,c}_{k+1|k+1} &= \hat{x}^{aug}_{k+1|k} + (P_{k+1|k}{}^{-1} + H^TR^{-1}H)^{-1}H^T \\ &\quad R^{-1}(y_{k+1} - H\hat{x}^{aug}_{k+1|k}) \\ &\quad -\frac{1}{2}(P_{k+1|k}{}^{-1} + H^TR^{-1}H)^{-1}E^T\lambda \end{aligned} \tag{26}$$

Following the definition of the Kalman gain matrix, K_{k+1}, in eq 9 and matrix inversion lemma,[16] we have

$$\begin{aligned} &[P_{k+1|k}{}^{-1} + H^TR^{-1}H]^{-1} \\ &= [P_{k+1|k}{}^{-1} + H^TR^{-1}H]^{-1}[I + H^TR^{-1}HP_{k+1|k} \\ &\quad - H^TR^{-1}HP_{k+1|k}] \\ &= [P_{k+1|k}{}^{-1} + H^TR^{-1}H]^{-1}[[P_{k+1|k}{}^{-1} + H^TR^{-1}H]P_{k+1|k} \\ &\quad - H^TR^{-1}HP_{k+1|k}] \\ &= P_{k+1|k} - [P_{k+1|k}{}^{-1} + H^TR^{-1}H]^{-1}H^TR^{-1}HP_{k+1|k} \\ &= P_{k+1|k} - K_{k+1}HP_{k+1|k} \\ &= P_{k+1|k+1} \end{aligned} \tag{27}$$

Substituting eq 27 into eq 26 and using the state update in eq 6, we have

$$\hat{x}^{aug,c}_{k+1|k+1} = \hat{x}^{aug}_{k+1|k+1} - \frac{1}{2}P_{k+1|k+1}E^T\lambda \tag{28}$$

Substituting eq 28 into eq 25 and solving for Lagrangian multiplier, λ, we get

$$\lambda = 2(EP_{k+1|k+1}E^T)^{-1}(E\hat{x}^{aug}_{k+1|k+1} - b) \tag{29}$$

Substituting the value of the Lagrangian multiplier from eq 29, the states are updated in the presence of equality constraints as

$$\hat{x}^{aug,c}_{k+1|k+1} = F\hat{x}^{aug}_{k+1|k+1} + b' \tag{30}$$

where

$$F = (I - P_{k+1|k+1}E^T(EP_{k+1|k+1}E^T)^{-1}E) \tag{31}$$

$$b' = P_{k+1|k+1}E^T(EP_{k+1|k+1}E^T)^{-1}b \tag{32}$$

where $P_{k+1|k+1}$ is the KF covariance matrix calculated similar to eq 8. Using the state propagation matrix, for the covariance matrix update we have

$$\begin{aligned} &P^c_{k+1|k+1} \\ &= FP_{k+1|k+1}F^T \\ &= (I - P_{k+1|k+1}E^T(EP_{k+1|k+1}E^T)^{-1}E)P_{k+1|k+1} \\ &\quad (I - P_{k+1|k+1}E^T(EP_{k+1|k+1}E^T)^{-1}E)^T \\ &= P_{k+1|k+1} - P_{k+1|k+1}[P_{k+1|k+1}E^T(EP_{k+1|k+1}E^T)^{-1}E]^T \\ &\quad - P_{k+1|k+1}E^T(EP_{k+1|k+1}E^T)^{-1}EP_{k+1|k+1} \\ &\quad + P_{k+1|k+1}E^T(EP_{k+1|k+1}E^T)^{-1}EP_{k+1|k+1} \\ &\quad [P_{k+1|k+1}E^T(EP_{k+1|k+1}E^T)^{-1}E]^T \\ &= P_{k+1|k+1} - P_{k+1|k+1}E^T(EP_{k+1|k+1}E^T)^{-1}EP_{k+1|k+1} \\ &\quad - P_{k+1|k+1}E^T(EP_{k+1|k+1}E^T)^{-1}EP_{k+1|k+1} \\ &\quad + P_{k+1|k+1}E^T(EP_{k+1|k+1}E^T)^{-1}(EP_{k+1|k+1}E^T)(EP_{k+1|k+1}E^T)^{-1} \\ &\quad EP_{k+1|k+1} \\ &= P_{k+1|k+1} - P_{k+1|k+1}E^T(EP_{k+1|k+1}E^T)^{-1}EP_{k+1|k+1} \\ &\quad - P_{k+1|k+1}E^T(EP_{k+1|k+1}E^T)^{-1}EP_{k+1|k+1} + P_{k+1|k+1}E^T \\ &\quad (EP_{k+1|k+1}E^T)^{-1}EP_{k+1|k+1} \\ &= P_{k+1|k+1} - P_{k+1|k+1}E^T(EP_{k+1|k+1}E^T)^{-1}EP_{k+1|k+1} \\ &= (I - P_{k+1|k+1}E^T(EP_{k+1|k+1}E^T)^{-1}E)P_{k+1|k+1} \\ &= FP_{k+1|k+1} \end{aligned} \tag{33}$$

Remark 2.3: Assume that equality constraint, E, in eq 10 can be split into $E = \begin{bmatrix} E_x \\ E_z \end{bmatrix}^T$, where $E_x \in \mathbb{R}^{l\times m}$ is the left eigenvector(s) of Φ that satisfies $E_xG = 0_{l\times m}$, $E_xf_x = 0_{m\times 1}$, and $E_z = 0_{l\times n}$, where f_x is the differential equation of the DAE system represented by eq 10. Also assume that, for a given $k = 1$, $E\hat{x}^{aug,c}_{k+1|k+1} = b$ and $EP^c_{k+1|k+1} = 0_{l\times m+n}$. Then, for all $k \geq 2$, $x^{aug,c}_{k+1|k+1} = \hat{x}^{aug}_{k+1|k+1}$ and $P^c_{k+1|k+1} = P_{k+1|k+1}$.

Proof: By multiplying the differential equations in the DAE system of eq 10 by E, we get

$$\begin{aligned} Ex^{aug}_{k+1} &= E_xx_k + \int_{k\Delta t}^{(k+1)\Delta t} E_xf_x(x(t), z(t))dt + E_xG\omega_{k+1} \\ &\quad + E_zz_{k+1} \\ &= b + 0_{l\times 1} + 0_{l\times 1} + 0_{l\times 1} \\ &= b \end{aligned} \tag{34}$$

Since E_x is the left eigenvector(s) of Φ, then we can write $E_x\Phi = \lambda E_x$, where λ's are the eigenvalues of the corresponding eigenvectors. Multiplying eq 15 by E then yields

DOI: 10.1021/acs.iecr.6b02796
Ind. Eng. Chem. Res. 2017, 56, 206−215

$$EP_{k+1|k} = \begin{bmatrix} E_x P^{xx}_{k+1|k} + E_z P^{zx}_{k+1|k} \\ E_x P^{xz}_{k+1|k} + E_z P^{zz}_{k+1|k} \end{bmatrix}^T$$
$$= \begin{bmatrix} (E_x \phi P^{xx}_{k|k} \phi^T + E_x G Q G^T) + E_z (D^{-1}C) P^{xx}_{k+1|k} \\ E_x P^{xx}_{k+1|k} (D^{-1}C)^T + (E_z (D^{-1}C) P^{xx}_{k+1|k} (D^{-1}C)^T + E_z M) \end{bmatrix}^T$$
$$= \begin{bmatrix} (\lambda E_x P^{xx}_{k|k} \phi^T + 0_{l\times m}) + 0_{l\times m} \\ 0_{l\times n} + (0_{l\times n} + 0_{l\times n}) \end{bmatrix}^T$$
$$= 0_{l\times(m+n)} \tag{35}$$

Lemma 2.1: let ν be a left eigenvector of the square matrix U with a corresponding eigenvalue λ. Then, $\nu e^{U\Delta t} = e^{\lambda \Delta t}\nu$.

Proof: To prove this, we can write $U\Delta t = U\Delta t - \lambda I \Delta t + \lambda I \Delta t$; therefore,

$$\nu e^{U\Delta t} = \nu e^{U\Delta t - \lambda I \Delta t + \lambda I \Delta t}$$
$$= \nu e^{(U-\lambda I)\Delta t + \lambda I \Delta t}$$
$$= \nu e^{(U-\lambda I)\Delta t} e^{\lambda \Delta t}$$
$$= \nu \left(I + (U - \lambda I)\Delta t + \frac{(U-\lambda I)^2 \Delta t^2}{2!} + \cdots \right) e^{\lambda \Delta t}$$
$$= \left(\nu I + \nu (U - \lambda I)\Delta t + \frac{\nu (U-\lambda I)^2 \Delta t^2}{2!} + \cdots \right) e^{\lambda \Delta t}$$
$$= (\nu I + 0 + 0 + \cdots) e^{\lambda \Delta t}$$
$$= e^{\lambda \Delta t} \nu \tag{36}$$

Therefore, in eq 35 E_x is already the left eigenvector(s) of $(A - BD^{-1}C)$. Multiplying eqs 30 and 33 by E yields

$$E\hat{x}^{aug,c}_{k+1|k+1} = EF\hat{x}^{aug}_{k+1|k+1} + Eb'$$
$$= E(I - P_{k+1|k+1}E^T(EP_{k+1|k+1}E^T)^{-1}E)\hat{x}^{aug}_{k+1|k+1}$$
$$+ EP_{k+1|k+1}E^T(EP_{k+1|k+1}E^T)^{-1}b$$
$$= (E - E)\hat{x}^{aug}_{k+1|k+1} + b$$
$$= b \tag{37}$$

$$EP^c_{k+1|k+1} = EFP_{k+1|k+1}$$
$$= E(I - P_{k+1|k+1}E^T(EP_{k+1|k+1}E^T)^{-1}E)P_{k+1|k+1}$$
$$= (E - E)P_{k+1|k+1}$$
$$= 0_{l\times(m+n)} \tag{38}$$

Given eqs 37−38, from eq 34−35, we have $x^{aug,c}_{k+1|k+1} = \hat{x}^{aug}_{k+1|k+1}$, and $P^c_{k+1|k+1} = P_{k+1|k+1}$. Therefore, if the assumptions hold, the correction step in eqs 30 and 33 has to be performed only once at $k = 1$, and for all $k \geq 2$ the corrected states given by eq 6 already satisfy $E\hat{x}^{aug}_{k+1|k+1} = b$.[17]

4. NUMERICAL RESULTS

In this section, the performance of the proposed state estimation technique is demonstrated on two examples. The first example is a nonlinear system that is akin to a batch reactor, and the second example is the water gas shift reactor (WGSR), where a catalytic reaction is performed in a plug-flow reactor. Before we proceed to describe the results, some remarks are in order. Convergence of the estimator is an important question that is not addressed in this work. Establishing convergence results for nonlinear filters is, in general, a difficult problem. Further, global observability conditions are difficult to establish for general nonlinear systems. In our work, we infer observability from the quality of estimation from different runs at different initializations. For simplicity, the performance of the filter is demonstrated by comparison of an average (100 runs) root-mean-square error (RMSE) of the data and the estimated states calculated as

$$RMSE = \sqrt{\frac{\sum_{i=1}^{s} (x_{i,k} - \hat{x}^c_{i,k})^2}{s}} \tag{39}$$

where $x_{i,k}$ is the actual value that is specific to the simulation study and $\hat{x}^c_{i,k}$ is the constrained state estimate. In order to calculate the RMSE of the measurement data, $\hat{x}^c_{i,k}$ in eq 39 is replaced by the measured value $y_{i,k}$. Another metric that is used in the following analysis is the normalized sum of squared errors (SSE) of all state estimates over the total time instance and is calculated as

$$SSE = \sum_{t=1}^{T} \sum_{i=1}^{X} \left(\frac{x_i(t) - \hat{x}_i(t)}{x_i(t)} \right)^2 \tag{40}$$

where T is the number of time instances, X is the number of variables, and $x_i(t)$ and $\hat{x}i(t)$ are the i^{th} actual and estimated states at the t^{th} time instance, respectively. It should be noted that, in the following studies, SSE values are calculated by averaging over 100-run Monte Carlo simulations.

4.1. Example 1: Nonlinear synthetic system. Our synthetic example is comprised of two differential equations and an algebraic equation. The aim of this example is to show the filter performance when the assumptions in Remark 2.3 are valid. The system under study is given as

$$\begin{bmatrix} \dot{x}_1 \\ \dot{x}_2 \end{bmatrix} = \begin{bmatrix} 8.69 \times 10^{-4} z(0.6 - x_1) - z \times 10^{-3} \left(x_1 - \frac{x_2}{2} \right) \\ 8.69 \times 10^{-4} z(0.4 - x_2) + z \times 10^{-3} \left(x_1 - \frac{x_2}{2} \right) \end{bmatrix} + G \begin{bmatrix} \omega_1 \\ \omega_2 \end{bmatrix} \tag{41}$$

$$g(x) = z^{0.3} + 0.5 x_1^3 z - 10 \frac{x_2}{z} = \gamma \tag{42}$$

where $G = \begin{bmatrix} 0.5 & -0.5 \\ -0.5 & 0.5 \end{bmatrix}$ and true initial state of $x_0 = [0.431 \quad 0.569 \quad 3.546]^T$. The sampling time is chosen as $\Delta t = 5$ s, and the state estimator is initialized with

$$Q = \begin{bmatrix} 2.5 \times 10^{-5} & 0 \\ 0 & 2.5 \times 10^{-5} \end{bmatrix}$$
$$W = 2.5 \times 10^{-3}$$
$$R = \begin{bmatrix} 2.5 \times 10^{-5} & 0 & 0 \\ 0 & 2.5 \times 10^{-5} & 0 \\ 0 & 0 & 2.5 \times 10^{-3} \end{bmatrix}$$
$$P_0 = \begin{bmatrix} 10^{-4} & 0 & 0 \\ 0 & 10^{-4} & 0 \\ 0 & 0 & 10^{-4} \end{bmatrix}$$
$$x_{0|0} = [0.555 \quad 0.456 \quad 2.822]^T \tag{43}$$

The constraint given for this system is

$$E = [1 \quad 1 \quad 0], \qquad b = 1 \tag{44}$$

DOI: 10.1021/acs.iecr.6b02796
Ind. Eng. Chem. Res. 2017, 56, 206−215

Note that the initial estimate does not satisfy the constraint. From the constraint it can be seen that $E_x = [1 \;\; 1]$, $E_z = 0_{1\times1}$, $E_xG = 0_{1\times2}$, and $E_xf_x = 0_{1\times1}$. The Jacobian matrix is calculated analytically as

$$\begin{bmatrix} A & B \\ C & D \end{bmatrix} = \begin{bmatrix} (-0.869z - z) \times 10^{-3} & -\frac{z}{2} \times 10^{-4} & \left(0.869(0.6 - x_1) - \left(x_1 - \frac{x_2}{2}\right)\right) \times 10^{-3} \\ z \times 10^{-3} & \left(-0.869z - \frac{z}{2}\right) \times 10^{-3} & \left(0.869(0.4 - x_2) + \left(x_1 - \frac{x_2}{2}\right)\right) \times 10^{-3} \\ 1.5x_1^2 z & \frac{-10}{z} & 0.3z^{-0.7} + 0.5x_1^3 + \frac{10x_2}{z^2} \end{bmatrix} \tag{45}$$

Multiplying E_x by $(A - BD^{-1}C)$ yields

$$\begin{aligned} & E_x(A - BD^{-1}C) \\ &= [1 \;\; 1] \begin{bmatrix} -8.69z \times 10^{-4} - z \times 10^{-3} + z \times 10^{-3} & -\frac{z}{2} \times 10^{-3} \\ z \times 10^{-3} & -8.69z \times 10^{-4} + \frac{z}{2} \times 10^{-3} \end{bmatrix} \\ &= [-86.9z \times 10^{-4} \;\; -86.9z \times 10^{-4}] \\ &= -86.9z \times 10^{-4} \times [1 \;\; 1] \end{aligned} \tag{46}$$

From eq 44, it is known that $x_1 + x_2 = 1$ after the first iteration of the filter; therefore, $E_xBD^{-1}C = 0$. From eq 46, E_x is a left eigenvector of Φ. Since the assumptions in Remark 2.3 hold, state estimates are obtained as explained in Remark 2.3. Figures 1−3 show the actual, measured, and estimated values

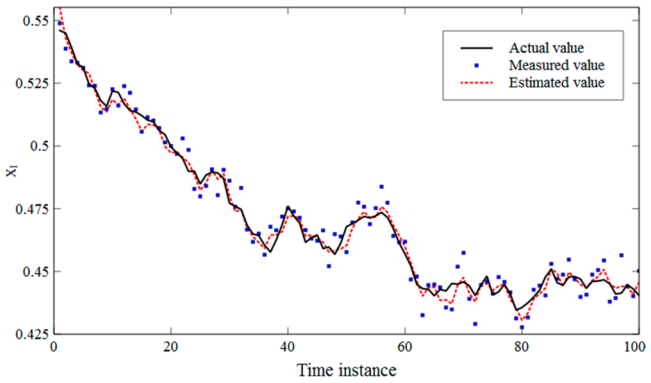

Figure 1. Actual, measured, and estimated values of differential variable x_1.

of each variable for 100 time instances. Initially, the states do not satisfy the constraint; however, after the first iteration of the filter, estimated states satisfy the constraints for all time instances.

In Table 1, RMSE and SSE values of measured and estimated variables are reported. The RMSE and SSE are compared for Filter I, filter with certain algebraic equation assumptions as described in Section 2, and Filter II, the proposed filter. It should be noted that the propagation step in Filter I is modified to include the state constraints as shown in eq 21. As seen in Table 1, RMSE of differential variables x_1 and x_2 using Filter II are slightly reduced over using Filter I and both filters result in

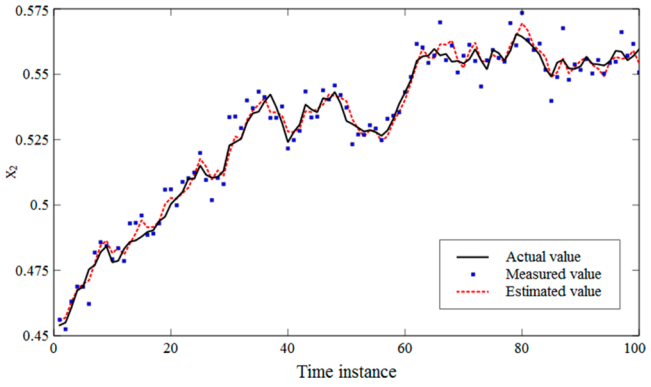

Figure 2. Actual, measured, and estimated values of differential variable x_2.

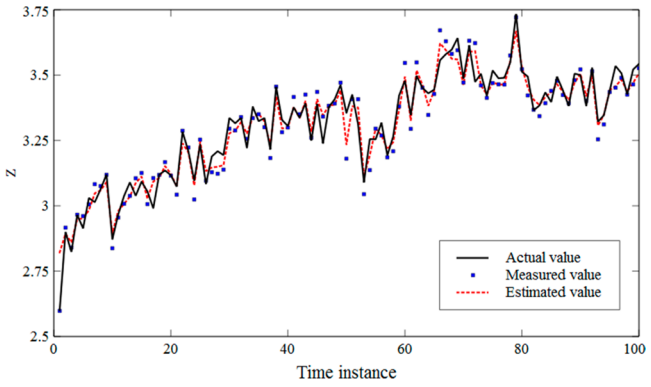

Figure 3. Actual, measured, and estimated values of algebraic variable z.

better estimates compared to the measurements. The RMSE of the algebraic variable z for Filter I is greater than that of the measurement due to underestimation of noise in its

DOI: 10.1021/acs.iecr.6b02796
Ind. Eng. Chem. Res. 2017, 56, 206−215

Table 1. Comparison of RMSE and SSE Values for Measured and Estimated Values

	RMSE (variance)			SSE
	x_1	x_2	z	
Measurement (data)	0.0050	0.0050	0.0501	
Filter I	0.0029 (6.99×10^{-8})	0.0029 (6.99×10^{-8})	0.0684 (2.00×10^{-5})	0.0479
Filter II	0.0027 (5.69×10^{-8})	0.0027 (5.69×10^{-8})	0.0417 (1.03×10^{-5})	0.0215

corresponding equation. This suggests that measuring the algebraic variable would result in more accurate values than using Filter I. However, the reduced RMSE of the algebraic variable for Filter II compared to the RMSE of the measurement justifies the correct assumption of uncertain algebraic equations. Also, the SSE value of Filter II indicates significant improvement over Filter I, which means the estimates are closer to the actual values. These improvements show that the proposed filter can mitigate the effect of uncertain algebraic equations and result in better estimates.

4.2. Example 2: Water gas shift reactor. State estimation in reactors has been the focus of many researchers for control and fault diagnosis. The next example is the system of interest, the water gas shift reactor (WGSR), in which carbon monoxide (CO) reacts with steam (H_2O) to produce hydrogen (H_2) and carbon dioxide (CO_2), through the water gas shift reaction. A nonlinear DAE model of the sour water gas shift reactor (SWGSR) has been developed in our previous work where, in addition to the water gas shift reaction, carbonyl sulfide (COS) reacts with H_2O (i.e., COS hydrolysis), and CO_2 and hydrogen sulfide (H_2S) are produced.[18] For simplicity, here, the sulfur content of the feed is assumed negligible and only the water gas shift reaction is considered. The reader is referred to our previous work for complete modeling of the reactor.[18] In addition to the reactor model, feed and product stream flow rates are controlled by valves (V_1, V_2, and V_3) as shown in Figure 4.

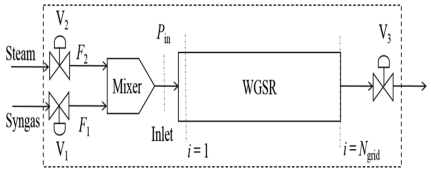

Figure 4. Schematic of the WGSR system.

The corresponding equation for calculation of flows through the valves is $F_{Vi} = \left(\frac{d_{V_i} S_{V_i}}{M_{V_i}}\right)\sqrt{\rho_{V_i} \Delta P_{V_i}}$, where d_{V_i}, S_{V_i}, M_{V_i}, ρ_{V_i}, and ΔP_{V_i} are the flow coefficient, valve opening, average molecular weight, average density, and pressure drop across the valve, respectively. Syngas and steam are passed through valves V_1 and V_2, respectively, and it is assumed that these streams are well mixed in an ideal mixer before entering the reactor. The presence of the valve adds an additional algebraic equation to the system model as described by eqs 47−51. Table 2 shows the summary of the equations used to represent the system with parameters shown in Table 3. Some of the parameters in our previous work are changed for simplicity and reduced computations. For example, the reactor size and correspondingly the number of grid points in the discretization are reduced. These parameters are shown in Table 3.

Table 3. Summary of the Parameters of the WGSR Model Used in This Work

Parameter		Value
Length		1 m
Diameter		0.5 m
Number of grids (N_{grid})		25
Valve V_1 (syngas)	Opening	50%
	Flow Coefficient	6×10^{-5}
Valve V_2 (steam)	Opening	50%
	Flow Coefficient	2×10^{-5}
Valve V_3 (products)	Opening	50%
	Flow Coefficient	10^{-4}
Inlet temperature		580 K
Feed pressure (steam and syngas)		5626121 Pa
Outlet pressure		4.5×10^{-5} Pa
Catalyst diameter		0.1 mm

Table 2. Summary of Equations for the Water Gas Shift Reactor

$$\frac{\partial y_i}{\partial t} = \frac{RT}{P}\left(-F_{MF}\frac{\partial y_i}{\partial z} + r_{WGS,i}\frac{1-\varepsilon}{\varepsilon}\right) + G\omega_{1,i} \quad (47)$$

$$i = \mathrm{CO},\ \mathrm{H_2O},\ \mathrm{CO_2 and\ H_2}$$

$$\frac{\partial T_g}{\partial t} = \frac{1}{\rho_{gas} C_p}\left[-C_p F_{MF}\frac{\partial T_g}{\partial z} + \frac{h_f a_c}{\varepsilon}(T_{cat} - T_{gas})\right] + \omega_2 \quad (48)$$

$$\frac{\partial T_{cat}}{\partial t} = \frac{1}{\rho_{cat} C_{p,cat}}\left[K_{cat}\frac{\partial^2 T_{cat}}{\partial z^2} - \frac{h_f a_c}{1-\varepsilon}(T_{cat} - T_{gas}) + r_{WGS}\rho_{cat}\Delta H_{R,WGS}\right] + \omega_3 \quad (49)$$

$$\frac{dP}{dz} = \frac{\rho u^2}{D_{cat}}\left(\frac{1-\varepsilon}{\varepsilon^3}\right)\left(1.75 + \frac{150}{Re}\right) + \gamma_1 \quad (50)$$

$$\Delta P_{V_3} = \frac{1}{\rho_{V_3}}\left(\frac{F_{V_3} M_{V_3}}{d_{V_3} S_{V_3}}\right)^2 + \gamma_2 \quad (51)$$

DOI: 10.1021/acs.iecr.6b02796
Ind. Eng. Chem. Res. 2017, 56, 206−215

The partial differential equations in eqs 47−49 are converted into ordinary differential equations by discretization along the reactor axis with N_{grid} number of grid-points, where the grid-points start from $\frac{L}{N_{grid}}$ meters from the reactor entrance. The state vector consists of 176 states including mole fractions of CO, H_2O, CO_2, and H_2, temperature, and pressure at each grid-point and pressure at the inlet of the reactor (P_{in}). The constraint for this system is imposed as the summation of mole fractions at each grid-point is equal to one. Since the actual mole fraction values must sum up to one for consistency, in simulating the actual mole fraction values, the process noise is introduced in the mole fractions in such a way that the summation of the process noises at each grid-point and time instance is equal to zero. To do this, random process noises generated for each mole fraction at a particular grid-point are corrected by subtracting the mean average of the process noise from each. Therefore, G in the system of eq 10 is written such the diagonal elements are $+\frac{3}{4}$ and the elements corresponding to the mole fractions of the other components at the same grid-point are $-\frac{1}{4}$. The process covariance, Q, of each equation type is assumed the same and chosen as 10^{-4} and 2.5×10^{-5} for mole fraction and temperature equations, respectively. The covariance matrix of the algebraic equations (pressure) is also fixed at 4×10^{-4}. The measurement covariance, R, is also assumed in the same manner with 6.4×10^{-5}, 2.5×10^{-5}, and 4×10^{-6} for mole fraction, temperature, and pressure measurements, respectively. It should be mentioned that the temperature and pressure variables are normalized using 580 K and 55 atm, respectively. The sampling time is chosen as $\Delta t = 5$ s, and the state estimation is performed for 100 time instances. The error covariance is $P_0 = 10^{-6} I_{176\times176}$. The condition in Remark 2.3 applies here also, and the correction step for the constraint is applied only once in the beginning. Note that since a large portion of the reactant is consumed in the first half of the reactor, it is more desirable to accurately estimate the states in this zone. Therefore, a random grid-point in the first half of the reactor is chosen to demonstrate the performance of the proposed filter. Figure 5 and Figure 6a show the actual, measured, and estimated states at the ninth grid-point using Filter II with all the states measured. The corresponding RMSE values along with the variances of the RMSE values of the estimated states using Filter II are shown in Table 4. For the sake of validation, the RMSE values for a different grid-point (18th grid-point) are also given in Table 4.

Clearly, the estimated values have smaller errors compared to the measurements; thus, the proposed filter performs as desired. It should be mentioned that, for better visualization, Figure 5 and Figure 6 are shrunk for the first 30 time instances, although the calculations of RMSE and SSE values are based on 100 time instances. In order to avoid comparing the RMSE of a large number of variables for Filter I and Filter II in this example, the superiority of the proposed filter, Filter II, is shown by comparing SSE values and also RMSE values at the ninth grid-point for the algebraic variable P. The SSE values are 10.312 and 6.819 for Filter I and Filter II, respectively. Comparing the SSE values, the proposed filter results in estimated values significantly closer to the actual values as the squared error is reduced approximately by 33%. Moreover, higher $RMSE_{est}$ for Filter I than $RMSE_{data}$ shows that the filter fails to outperform the measurements and produce unreliable estimates while Filter II results in estimates with lower errors

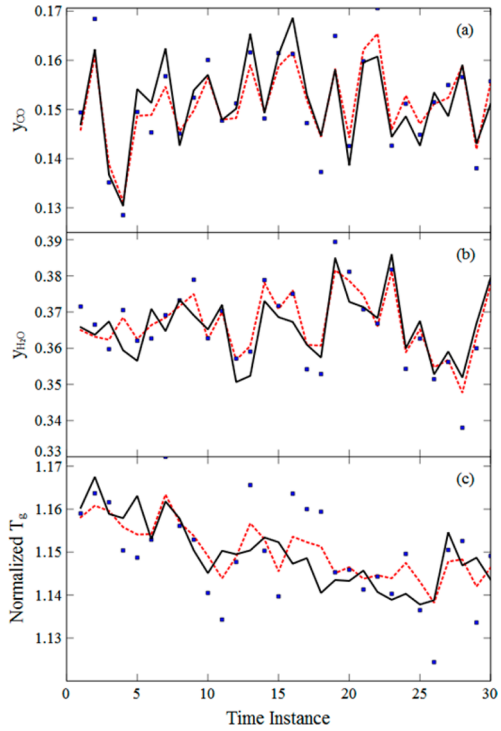

Figure 5. Actual (−), measured (*), and estimated (--) value at the 9th grid-point on the reactor for (a) y_{CO}, (b) y_{H_2O}, and (c) T_g.

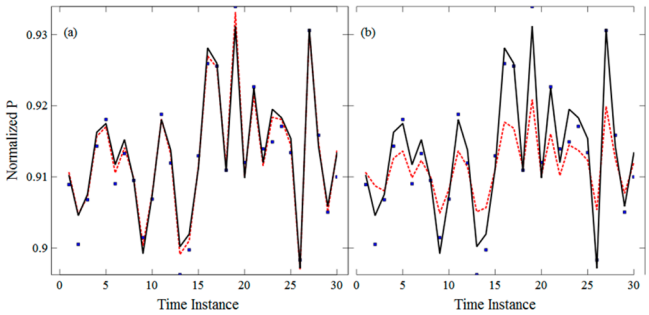

Figure 6. Actual (−), measured (*), and estimated (--) value at the 9th grid-point on the reactor for (a) P (using Filter II) and (b) P (using Filter I).

than that of measurements. The state estimation results are presented in Figure 6a and Figure 6b for Filter II and Filter I, respectively. From Figure 6, it can be seen how accurately Filter II tracks the changes in the algebraic state compared to Filter I. As mentioned before, this is due to the fact that Filter II correctly accounts for the presence of noise in the algebraic state. Consequently, this is reflected in the quality of the state estimates. In terms of the computational effort, although in updating the error covariance matrix, different blocks of the predicted covariance and the Jacobian matrix are used, the computational complexity of the calculations remains fairly the same; therefore, using the proposed filter will show similar computational time as if the EKF was used on an explicit ODE system. Further, in the proposed approach, the optimization problem is unconstrained and, hence, we have not addressed terminal constraints. There are several approaches for including constraints within the genetic algorithm framework explained in part 2 of this two-part series of papers, which can be explored to address this issue.

DOI: 10.1021/acs.iecr.6b02796
Ind. Eng. Chem. Res. 2017, 56, 206−215

Table 4. RMSE Values at the 9th and 18th Grid-Points on the Reactor

		RMSE (variance)		
	Grid-point	Measurement	Filter I	Filter II
y_{CO}	9th	5.005×10^{-3}	3.852×10^{-3} (8.537×10^{-8})	3.852×10^{-3} (8.524×10^{-8})
	18th	4.973×10^{-3}	3.877×10^{-3} (8.958×10^{-8})	3.877×10^{-3} (8.946×10^{-8})
y_{H_2O}	9th	5.003×10^{-3}	3.827×10^{-3} (7.940×10^{-8})	3.827×10^{-3} (7.954×10^{-8})
	18th	4.993×10^{-3}	3.897×10^{-3} (6.311×10^{-8})	3.896×10^{-3} (6.303×10^{-8})
T_g	9th	7.978×10^{-3}	4.958×10^{-3} (1.237×10^{-7})	4.945×10^{-3} (1.244×10^{-7})
	18th	7.914×10^{-3}	4.847×10^{-3} (1.520×10^{-7})	4.834×10^{-3} (1.493×10^{-7})
P	9th	1.998×10^{-3}	5.312×10^{-3} (1.415×10^{-7})	0.894×10^{-3} (0.452×10^{-9})
	18th	1.993×10^{-3}	5.588×10^{-3} (1.669×10^{-7})	0.883×10^{-3} (0.391×10^{-9})

5. DISCUSSION

In the previous section, our proposed filter, which accurately estimates the states, especially the algebraic states, was used to estimate the states in the WGSR example. In the WGSR example, however, all the states are measured for the purpose of filtering. Practically, it is neither possible nor economical to measure all the states in the WGSR. In operating plants, as the budget and integrity of the equipment items limit the number and type of sensors that can be used for monitoring the process, state estimation becomes a challenge. Increasing the number of sensors results in more accurate estimates of the variables. On the other hand, reducing the number of sensors requires identifying the most important variables that, if measured, would provide accurate state estimates. However, the following questions arise. What should be the type and location of the sensors? How much does each measurement type and location contribute to the accuracy of the state estimates, especially when using a rigorous filter for state estimation? To answer these questions, we begin by evaluating the case where only a few measurements are available. First, it is assumed that measurements are mutually exclusive and only available at fixed locations for similar states (i.e., only mole fractions of CO, y_{CO}, or, only gas temperature, T_g, at fixed locations). The fixed grid-points are assumed to be first, fifth, ninth, 13th, 17th, and 21st grid-points. For satisfying product specification, product concentration, temperature, and pressure are usually monitored at the reactor outlet. Therefore, in subsequent studies it is assumed that all the states except the catalyst temperature, T_{cat}, are always measured at the outlet of the reactor (25th grid-point). Table 5 shows the SSE values for the corresponding available measurements with $T = 100$. As seen in Table 5, the lowest estimation error is achieved if the measurements of CO mole fraction (y_{CO}) are available. In contrast, if measurements of only pressure (P) are available, estimation error is comparatively higher than others in Table 5. Therefore, it can be concluded that the type of the variable that is being measured contributes to the accuracy of the estimation, and if identified, it can result in better estimation accuracy.

Table 5. Sum of Squared Error Values When Fixed Points Measure the Same Type of States

	Measured state type					
	y_{CO}	y_{H_2O}	y_{CO_2}	y_{H_2}	T_g	P
SSE value	31.889	35.522	34.626	35.500	36.077	37.790

Next, we investigate how informative are each of the fixed measurement locations when only y_{CO} is measured. Therefore, six independent cases are considered, where in each case it is assumed that one of the measurement locations is unavailable and information from only five other measurement locations is used for state estimation. Table 6 shows the SSE values for each of these state estimations with $T = 100$. Table 6 shows that the 13th, 17th, and 21st grid-points have the highest impact on the accuracy of the estimates with approximately minimum 3% increase in the overall squared estimation error in the absence of measurements from each of these grid-points individually. Moreover, even with one less measurement of y_{CO}, measurement of y_{CO} results in better estimation accuracy in comparison to the cases where temperature or pressure are measured. Next we investigate if measurements from other variables at different locations combined with measurements of y_{CO} can actually improve the accuracy of the estimates while the total number of locations is still six. For this study, y_{CO} measurements from the 13th and 17th, and 21st grid-points, which have the highest impact on the accuracy, are combined with measurements of temperature and y_{H_2O}.

Table 7 shows SSE values when combinations of variables are measured at different locations. Since the number of

Table 7. SSE Values with Measurement Combination

Iteration	Locations	SSE value
1	T_g[21] y_{CO_2}[13] y_{H_2O}[5]	32.160
2	T_g[5] y_{CO_2}[9] y_{H_2O}[5]	31.685
3	T_g[13] y_{CO_2}[5] y_{H_2O}[21]	32.087
4	T_g[9] y_{CO_2}[13] y_{H_2O}[21]	31.966
5	T_g[5] y_{CO_2}[13] y_{H_2O}[17]	31.906
6	T_g[9] y_{CO_2}[17] y_{H_2O}[1]	32.035
7	T_g[5,13] y_{CO_2}[17]	31.964
8	T_g[13] y_{CO_2}[5,9]	31.493
9	T_g[21] y_{CO_2}[1,17]	32.003
10	T_g[17] y_{CO_2}[5,21]	32.325
11	T_g[5] y_{CO_2}[1,21]	31.432
12	T_g[17] y_{CO_2}[9,21]	31.931

Table 6. Sum of Squared Errors with One Missing Measurement

	Removed measurement location						
	None	1st	5th	9th	13th	17th	21st
SSE value	31.889	32.119	32.171	32.439	32.982	33.315	33.572

DOI: 10.1021/acs.iecr.6b02796
Ind. Eng. Chem. Res. 2017, 56, 206−215

combinations of the type and locations is large, only a few combinations are considered and shown in Table 7. Interestingly, combinations 2, 8, and 11 show improvement over when only y_{CO} is measured. Moreover, in practice, if a measurement of y_{CO} can be replaced by a temperature measurement that is significantly cheaper, a considerable reduction in cost can be achieved. This means that not only the type of the measured variable contributes to the accuracy of the state estimates, the location where each of these variables are measured also contributes to the accuracy of the estimated values. However, if one were to consider all of the grid-points on the WGSR as candidate locations and pick the location and type of the variables with fixed total number of variables, a large number of combinations need to be evaluated. This motivates further research on the development of systematic ways to answer the question: what are the best types and locations of sensors on WGSR in order to generate the most accurate estimates with a limited budget.

6. CONCLUSION

Previous EKF frameworks for DAE systems published in the literature assume that algebraic equations are exact. However, in practice, algebraic equations could be describing a physical state and derived using modeling assumptions which introduce uncertainties in these process equations. However, stochastic algebraic equations cannot be handled in the previous EKF formulations due to differentiation of white noise which is not well-defined. Moreover, extra information about the process may be present in the form of implicit equality constraints, such as mole balance in a reactor, which should also be included in the framework as algebraic equations with no uncertainty. A modification to the EKF approach that addresses these difficulties by avoiding the differentiation of the algebraic equations is proposed. The performance of the proposed filter is demonstrated through two examples. In the simple example, it is shown that estimates are improved over the measurements as RMSE of estimated states are considerably reduced in comparison to the RMSE of the measured data. In the WGSR example, the filter also shows considerably higher estimation accuracy of the states over the measurements when all states are measured. In both examples, the proposed filter shows superiority over the previous filtering framework by returning estimates with lower RMSE and closer to the actual values. Application of the proposed filter to the WGSR revealed that the type and location of the sensors used on the WGSR have an important role in the accuracy of the state estimates.

AUTHOR INFORMATION

Corresponding Author

*Tel: 1-806-742-1765, Fax: 1-806-742-3552, E-mail address: raghu.rengasamy@ttu.edu.

ORCID

Parham Mobed: 0000-0003-4546-3861

Notes

The authors declare no competing financial interest.

ACKNOWLEDGMENTS

The authors gratefully acknowledge support from DOE through grant no. DE-FE0005749, titled "Model-Based Sensor Placement for Component Condition Monitoring and Fault Diagnosis in Fossil Energy Systems".

REFERENCES

(1) Kumar Mandela, R.; Rengaswamy, R.; Narasimhan, S.; Sridhar, L. N. Recursive State Estimation Techniques for Nonlinear Differential Algebraic Systems. *Chem. Eng. Sci.* **2010**, *65* (16), 4548−4556.

(2) Simon, D. Kalman Filtering With State Constraints a Survey of Linear and Nonlinear Algorithms. *IET Control Theory Appl.* **2010**, *4* (8), 1303−1318.

(3) Petzold, L. Differential/Algebraic Equations are not ODE's. *SIAM J. ScI. STAT. Comput.* **1982**, *3* (3), 367−384.

(4) Takamatsu, M.; Iwata, S. Index Reduction for Differential-Algebraic Equations by Substitution Method. *Linear Algebra Appl.* **2008**, *429* (8), 2268−2277.

(5) Chisci, L.; Zappa, G. Square-Root Kalman Filtering of Descriptor Systems. *Syst. Control Lett.* **1992**, *19* (4), 325−334.

(6) Darouach, M.; Boutayeb, M.; Zasadzinski, M. Kalman Filtering for Continuous Descriptor Systems. *Proc. 1997 Am. Control Conf.* **1997**, *3*, 2108−2112.

(7) Darouach, M.; Bassong Onana, a.; Zasadzinski, M. State Estimation of Stochastic Singular Linear Systems: Convergence and Stability. *Int. J. Syst. Sci.* **1993**, *24* (5), 1001−1008.

(8) Dai, L. State Estimation Schemes for Singular Systems. In *Preprints of the 10th IFAC World Congress*; Munich, Germany, 1987.

(9) Deng, Z.-L.; Liu, Y.-M. Descriptor Kalman Estimators. *Int. J. Syst. Sci.* **1999**, *30* (11), 1205−1212.

(10) Nikoukhah, R.; Willsky, A. S.; Levy, B. C.; Member, S. Kalman Filtering and Riccati Equations for Descriptor Systems. *IEEE Trans. Autom. Control* **1992**, *37* (9), 1325−1342.

(11) Becerra, V. M.; Roberts, P. D.; Gri, G. W.; Park, C.; Oax, C. C. B. Applying the Extended Kalman Filter to Systems Described by Nonlinear Differential-Algebraic Equations. *Control Eng. Pract* **2001**, *9* (3), 267−281.

(12) Åström, K. J. *Introduction to Stochastic Control Theory*; Courier Corporation: 2012.

(13) Campbell, S. L. Descriptor Systems in the 90s. 29th. *IEEE Decis. Contr. P.* **1990**, 442−447.

(14) Schon, T.; Gerdin, M.; Glad, T.; Gustafsson, F. A Modeling and Filtering Framework for Linear Differential-Algebraic Equations. *42nd IEEE Int. Conf. Decis. Control* **2003**, *1* (3), 892−897.

(15) Vachhani, P.; Rengaswamy, R.; Gangwal, V.; Narasimhan, S. Recursive Estimation in Constrained Nonlinear Dynamical Systems. *AIChE J.* **2005**, *51* (3), 946−959.

(16) Bernstein, D. S. *Matrix Mathematics: Theory, Facts, and Formulas*; Princeton University Press: 2009.

(17) Teixeira, B. O. S.; Chandrasekar, J.; Tôrres, L. a. B.; Aguirre, L. a.; Bernstein, D. S. State Estimation for Linear and Non-Linear Equality-Constrained Systems. *Int. J. Control* **2009**, *82* (5), 918−936.

(18) Mobed, P.; Maddala, J.; Rengaswamy, R.; Bhattacharyya, D.; Turton, R. Data Reconciliation and Dynamic Modeling of a Sour Water Gas Shift Reactor. *Ind. Eng. Chem. Res.* **2014**, *53* (51), 19855−19869.

DOI: 10.1021/acs.iecr.6b02796
Ind. Eng. Chem. Res. 2017, 56, 206−215